

# CIRCUMSTELLAR EMISSION FROM TYPE Ib AND Ic SUPERNOVAE

Roger A. Chevalier<sup>1</sup> and Claes Fransson<sup>2</sup>

## ABSTRACT

The presumed Wolf-Rayet star progenitors of Type Ib/c supernovae have fast, low density winds and the shock waves generated by the supernova interaction with the wind are not expected to be radiative at typical times of observation. The injected energy spectrum of radio emitting electrons typically has an observed index  $p = 3$ , which is suggestive of acceleration in cosmic ray dominated shocks. The early, absorbed part of the radio light curves can be attributed to synchrotron self-absorption, which leads to constraints on the magnetic field in the emitting region and on the circumstellar density. The range of circumstellar densities inferred from the radio emission is somewhat broader than that for Galactic Wolf-Rayet stars, if similar efficiencies of synchrotron emission are assumed in the extragalactic supernovae. For the observed and expected ranges of circumstellar densities to roughly overlap, a high efficiency of magnetic field production in the shocked region is required ( $\epsilon_B \approx 0.1$ ). For the expected densities around a Wolf-Rayet star, a nonthermal mechanism is generally required to explain the observed X-ray luminosities of Type Ib/c supernovae. Although the inverse Compton mechanism can explain the observed X-ray emission from SN 2002ap if the wind parameters are taken from the radio model, the mechanism is not promising for other supernovae unless the postshock magnetic energy density is much smaller than the electron energy density. In some cases another mechanism is definitely needed and we suggest that it is X-ray synchrotron emission in a case where the shock wave is cosmic ray dominated so that the electron energy spectrum flattens at high energy. More comprehensive X-ray observations of a Type Ib/c supernova are needed to determine whether this suggestion is correct.

*Subject headings:* stars: circumstellar matter — stars: mass loss — supernovae

---

<sup>1</sup>Department of Astronomy, University of Virginia, P.O. Box 400325, Charlottesville, VA 22904-4325; rac5x@virginia.edu

<sup>2</sup>Department of Astronomy, Stockholm University, AlbaNova, SE-106 91 Stockholm, Sweden

## 1. INTRODUCTION

SNe Ib/c (Type Ib and Ic supernovae) are hydrogen free, or nearly hydrogen free, and are thought to have stripped massive star core, i.e. Wolf-Rayet star, progenitors. The observed rate of SNe Ib/c indicates that they make up about 1/4 of massive star supernovae (e.g., Dahlén & Fransson 1999) and thus are an important mode of massive star death. Although single very massive stars may end their lives as Wolf-Rayet stars, they are probably not in sufficient numbers to account for all of the SNe Ib/c (Wellstein & Langer 1999); binary progenitors are likely to be important contributors to the rate.

Considerable interest in SNe Ib/c has been generated by their relation to GRBs (gamma-ray bursts). The spatial and temporal correlation of the Type Ic SN 1998bw with the burst GRB 980425 led to the probability of a chance superposition of only  $10^{-4}$  (Galama et al. 1998), and the extraordinary energy displayed by the optical (Iwamoto et al. 1998) and radio (Kulkarni et al. 1998) emission from the supernova made the identification even more secure. The case was clinched by the finding of Type Ic supernovae similar to SN 1998bw in the cosmological GRBs 030329 and 031203 (Stanek et al. 2003; Malesani et al. 2004). The broad line character of the optical spectrum of SN 1998bw, with velocities up to  $60,000 \text{ km s}^{-1}$ , led to the view that SNe Ib/c with such broad lines were likely to be related to GRBs, including SN 2002ap (Mazzali et al. 2002). However, SN 2002ap was a relatively weak radio (Berger, Kulkarni, & Chevalier 2002) and X-ray source. On the basis of the radio emission, Berger, Kulkarni, & Chevalier (2002) argued that the energy in high velocity ejecta was low, so that a connection to GRBs was unlikely for this object.

Although it is not known which SNe Ib/c have a GRB connection, it is clear at least some of them do and this led to the prediction that late radio observations of SNe Ib/c could yield the detection of an off-axis GRB jet that slowed down and radiated more isotropically (Paczyński 2001). Searches for such emission were undertaken (Stockdale et al. 2003; Berger et al. 2003; Soderberg et al. 2006a), leading to the detection of luminous radio and X-ray emission from SN 2001em (Stockdale et al. 2004), SN 2003L (Soderberg et al. 2005), and SN2003bg (Soderberg et al. 2006b). In the case of SN 2003L, broad-lined optical emission is not present (Matheson et al. 2003), and in no case is there direct evidence for a GRB connection. SNe Ib/c were generally not detected at radio wavelengths, showing that such luminous supernovae are rare (Soderberg et al. 2006a).

Although there have been discussions of the radio and X-ray emission from individual SNeIb/c, there has been little discussion of their overall properties and how they relate to the mass loss properties of the progenitor star. We consider these properties and discuss the mechanisms for X-ray emission from the supernovae. In § 2, the observed properties of SNe Ib/c are briefly reviewed. The hydrodynamics of the interaction and the resulting

velocities are estimated in § 3. The expected relativistic electron spectrum, allowing for loss processes, is treated in § 4 and the resulting synchrotron radio emission in § 5. The possible mechanisms for the X-ray emission and their application to the observations are discussed in § 6. A discussion of the results is in § 7.

## 2. OBSERVED PROPERTIES

Clear signs of circumstellar interaction in SNe Ib/c are not present at optical wavelengths, but are seen at radio and X-ray wavelengths. Radio light curves have been observed for SN 1983N (Weiler et al. 1986), SN 1984L (Panagia, Sramek, & Weiler 1986), SN 1990B (Van Dyk et al. 1993), SN 1994I (Stockdale et al. 2005), SN 1998bw (Kulkarni et al. 1998), SN 2001ig (Ryder et al. 2004), SN 2002ap (Berger, Kulkarni, & Chevalier 2002), SN 2003L (Soderberg et al. 2005), and SN 2003bg (Soderberg et al. 2006b). SN 2001ig was observed to have H lines in its spectrum at one point, but some of its properties point to a Wolf-Rayet star progenitor (Ryder et al. 2004; Soderberg et al. 2006b), so we include it here.

The light curves for the radio supernovae show an early increase followed by a decline. The peak spectral luminosity and time of peak for various supernovae are shown in Fig. 2 of Chevalier, Fransson, & Nymark (2006). If SSA (synchrotron self-absorption) is the dominant absorption process, the position of the supernovae in this plot gives an indication of the velocity of the radio emitting shell (Chevalier 1998). SNe Ib/c generally separate themselves from other supernovae in this plot by having high velocities. The Type Ic SN 1998bw, associated with GRB 980425, stands out even more by requiring relativistic motion. Other Type Ic supernovae associated with GRBs, e.g., SN 2003dh with GRB 030329 and SN 2003lw with GRB 031203, had radio properties indicating highly relativistic motion. In these last two cases, the radio emission is generally believed to be associated with power from the same central engine that caused the GRB. The case of SN 1998bw has been more controversial. Li & Chevalier (1999) suggest an association with the GRB power source, but others have argued for a supernova origin for the radio and X-ray emission (Waxman 2004). Other than SN 1998bw, we do not treat the SNe Ic associated with GRBs here.

One quantity of interest that can be found from radio observations in the optically thin regime is the energy spectral index of the synchrotron emitting electrons. The values of  $\alpha$ , where  $F_\nu \propto \nu^\alpha$ , are given in Table 1. These values cover a range of times, but go to as late as several hundred days in some cases. The corresponding energy spectral index is  $p = -2\alpha + 1 \approx 3$  for these supernovae. The spectral indices are generally steeper for the SNe Ib/c than for other types of supernovae. Table 1 also gives  $\beta$ , where  $F_\nu \propto t^\beta$ , in the optically thin regime. The uncertainties in these values are  $\sim 0.1 - 0.2$  and vary among

the different objects. There are only a few data points for SN 1984L, so those results are especially uncertain. SN 2001ig and SN 2003bg both showed jumps in their light curves; the numbers used here do not include those parts of the light curves.

SNe Ib/c generally have no more than a few X-ray observations, so there is no complete light curve information. Table 2 lists the current observations, including the unabsorbed luminosities, of SNe Ib/c; all the detections are of Type Ic objects, which are the ones without He lines. The distances in Table 2 and 3 are based on  $H_0 = 70 \text{ km s}^{-1} \text{ Mpc}^{-1}$ . For SN 2003L and SN 2003bg, the distances are based on the recession velocity of the host galaxy and this value of  $H_0$ ; in all the other cases, the distances of Tully & Fisher (1988) have been scaled to  $H_0 = 70$  from their assumed value of 75. The resulting distance to SN 2002ap, 10.4 Mpc, is at the high end of the range of distances typically chosen for this supernova, but we are especially interested in having a consistent set of relative distances. SN 1994I in M51 was detected by *Chandra* at an age of  $\sim 7$  years (Immler, Wilson, & Terashima 2002); apparently it was detected at a later age in X-rays than in any other wavelength band.

### 3. HYDRODYNAMICS

The hydrodynamic interaction between a supernova and its surroundings depends on the density structure of the freely expanding supernova ejecta and the structure of the circumstellar medium. If SNe Ib/c have Wolf-Rayet progenitors, typical wind properties are  $\dot{M} \approx 10^{-5} M_\odot \text{ yr}^{-1}$  and  $v_w \approx 1000 \text{ km s}^{-1}$ . We define a constant to specify the wind density  $\rho = Ar^{-2} = \dot{M}/4\pi r^2 v_w$ , with a reference value  $A_* = A/(5 \times 10^{11} \text{ g cm}^{-3})$  corresponding to the typical wind properties. Because of the high wind velocity, the supernova shock samples a region of recent mass loss, so the assumption of steady mass loss and a  $r^{-2}$  density profile is reasonable. For the mass loss rates and wind velocities determined by Nugis & Lamers (2000) for Galactic Wolf-Rayet stars,  $A_*$  ranges from 0.07 – 7.4. The low value is for a WO star with  $v_w = 5,500 \text{ km s}^{-1}$ . If the supernova shock moves out at  $30,000 \text{ km s}^{-1}$  and the wind velocity is  $1000 \text{ km s}^{-1}$ , then the age of the wind that is sampled by the supernova is  $30t$ , where  $t$  is the age of the supernova. Since  $t$  is typically  $<$  a few years for observed SNe Ib/c, the radio emission is sensitive to changes in the mass loss properties on only a short timescale before the explosion ( $\lesssim 10^2$  yr). If a slow wind were present from an earlier evolutionary phase, a longer timescale for change would be possible because of the slower wind velocity; this may have occurred in the Type Ib/c SN 2001em (Chugai & Chevalier 2006). We do not discuss that situation any further here.

A number of studies of SNe Ib/c have quoted mass loss rates assuming a wind velocity of  $10 \text{ km s}^{-1}$  (e.g., Van Dyk et al. 1993; Immler, Wilson, & Terashima 2002; Ryder et al.

2004). A rationale for a low velocity is that the wind is from a late type companion with a slow wind. However, the ram pressure of a Wolf-Rayet star wind is likely to dominate that of any companion star. Van Dyk et al. (1993) address this by suggesting that SNe Ib/c are the thermonuclear explosions of cores. The further study of SNe Ib/c has supported the Wolf-Rayet hypothesis for their progenitors and we assume a fast wind here. When they occur in binary systems, the Wolf-Rayet wind can sweep back the companion star wind. The spiral structure that then results from the binary motion has been observed in some Wolf-Rayet systems (Tuthill, Monnier, & Danchi 1999).

The supernova structure depends on explosion models. Matzner & McKee (1999) discussed the density profiles resulting from the explosions of stars with radiative envelopes, as expected for SNe Ib/c progenitors. Radiative losses at the time of shock breakout set the upper limit to the velocity of the material that is shock accelerated at the outer edge of the star. The maximum velocity can be expressed as

$$v_{fmax} = 115,000 E_{51}^{0.58} \left( \frac{M}{10 M_{\odot}} \right)^{-0.42} \left( \frac{R_*}{1 R_{\odot}} \right)^{-0.32} \text{ km s}^{-1}, \quad (1)$$

where  $E$  is the explosion energy in units of  $10^{51}$  ergs,  $M$  is the ejecta mass,  $R_*$  is the progenitor radius ( $1 R_{\odot}$  is typical for a Wolf-Rayet star), and typical values have been used for the opacity and the progenitor density structure.

The resulting density profile, approximately a steep outer power law and a shallow inner power law, can be scaled with the ejecta mass,  $M$ , and energy  $E$ . Models of the optical light curves and spectra of particular supernovae lead to estimates of  $M$  and  $E$ . The outer density structure can be written as (Berger, Kulkarni, & Chevalier 2002)

$$\rho_{sn} = 3 \times 10^{96} E_{51}^{3.59} \left( \frac{M}{10 M_{\odot}} \right)^{-2.59} t^{-3} v^{-10.18}, \quad (2)$$

where  $v = r/t$  for the freely expanding gas and cgs units are used for the coefficient.

The interaction of the steep outer power law structure with the surrounding wind can be described by a self-similar solution for a  $\gamma = 5/3$  fluid (Chevalier 1982a). The solution should apply at early times and can be used to find the radius of the contact discontinuity between the ejecta and the circumstellar gas,  $R_c$ ,

$$\frac{R_c}{t} = 3.0 \times 10^4 E_{51}^{0.43} \left( \frac{M}{10 M_{\odot}} \right)^{-0.32} A_*^{-0.12} t_{10}^{-0.12} \text{ km s}^{-1}, \quad (3)$$

where  $t_{10}$  is the age in units of 10 days. The forward shock is at  $1.24R_c$  and the reverse shock at  $0.984R_c$ . The density at the reverse shock is 29 times that at the forward shock and the

mass of shocked ejecta is 2.0 times that of swept up circumstellar medium. In this solution, the fraction of the volume within the outer shock wave occupied by shocked gas is  $f = 0.50$ , which is made up of shocked circumstellar gas ( $f = 0.47$ ) and shocked ejecta ( $f = 0.03$ ).

Combining equations (1) and (3) gives the approximate time at which interaction with the power law profile begins

$$t_m = 0.0014 E_{51}^{-1.17} \left( \frac{M}{10 M_\odot} \right)^{0.83} A_*^{-1} \left( \frac{R_*}{1 R_\odot} \right)^{2.67} \text{ day.} \quad (4)$$

This is earlier than the time at which radio supernovae are observed, so the initial hydrodynamic evolution is expected to be in the self-similar regime of interaction with a steep power law. Deviations from self-similar behavior are expected when the reverse shock front moves into the interior, flatter part of the supernova density profile. To estimate the importance of this effect, we use the harmonic mean density distribution of Matzner & McKee (1999). Results for a particular density profile can be scaled to any appropriate values of stellar mass,  $M$ , explosion energy,  $E$ , and circumstellar density,  $A$ , using the scaling laws that lengths  $\sim M/A$  and time  $\sim M^{3/2} E^{-1/2} A^{-1}$ , so that  $v \propto (E/M)^{1/2}$ ,  $\rho \propto (A^3/M^2)$ , and  $p \propto A^3 E/M^3$ . We use results for the interaction in the thin shell approximation, as described by Chevalier (2005). These results show that at an age

$$t_e = 19 E_{51}^{-0.5} \left( \frac{M}{10 M_\odot} \right)^{1.5} A_*^{-1} \text{ yr,} \quad (5)$$

the value of  $m = (dR/dt)t/R = 0.866$ , corresponding to  $n = 9.5$ . This value is close to the initial value, so that the assumption of self-similar evolution over the time of observation of radio supernovae (at most up to a few years old) is a reasonable approximation.

The density structure advocated here can be compared to that found by other groups. The model CO100 has been used by Mazzali and collaborators to model energetic Type Ic supernovae (see Fig. 8 of Mazzali, Iwamoto, & Nomoto 2000, for the density structure). The high velocity ( $> 25,000 \text{ km s}^{-1}$ ) end of this structure can be approximated by a steep power law ( $\rho \propto r^{-9.0}$ ), in reasonable agreement with the model used here. However, Mazzali, Iwamoto, & Nomoto (2000) find that the spectroscopic modeling of the broad-line Type Ic SN 1997ef is improved by having a relatively flat density profile ( $\rho \propto r^{-4}$ ) over the velocity range  $25,000 - 50,000 \text{ km s}^{-1}$ . If the reverse shock wave of the interaction region propagated into such a shallow density gradient, the forward shock wave would begin to evolve toward  $R \propto t^{2/3}$  blast wave expansion.

Although the self-similar solution is expected to be adequate for the typical case, there may be circumstances where it fails. One is if there is a combination of high  $E$ , low  $M$ , and low  $A_*$  so that the flow is relativistic; this requires  $\beta\Gamma \approx 1$ , where  $\beta = v/c$  and  $\Gamma =$

$(1 - \beta^2)^{-1/2}$ , or  $v \approx 210,000 \text{ km s}^{-1}$  in equation (3). Tan et al. (2001) have discussed the supernova structure for the case where the accelerating shock at the outer edge of the star becomes relativistic. However, equation (3) shows that even for  $E_{51} = 10$  the shock velocity is not relativistic for radio and X-ray supernovae at typical times of observation. Another circumstance is recent change from a different stellar evolutionary phase, as described above.

Deviations from the  $\gamma = 5/3$  energy-conserving self-similar solution are expected if radiative cooling of the gas is important. For the hydrodynamic model described above, the velocity of gas moving into the reverse shock is

$$V_{rs} = 3.36 \times 10^3 E_{51}^{0.43} \left( \frac{M}{10 M_\odot} \right)^{-0.32} A_*^{-0.12} t_{10}^{-0.12} \text{ km s}^{-1}, \quad (6)$$

and the preshock density is

$$\rho_{rs} = 1.44 \times 10^{-18} E_{51}^{-0.87} \left( \frac{M}{10 M_\odot} \right)^{0.63} A_*^{1.24} t_{10}^{-1.76} \text{ g cm}^{-3}. \quad (7)$$

Unless the ejecta are very heavy element rich, the radiative cooling is dominated by free-free emission (see § 6.1) and the cooling time is larger than the age of the supernova even at  $t = 1$  day. The temperature gradually declines with time, but the density also declines and the cooling time remains larger than the age. The temperature at the outer shock is higher and density lower, so the cooling times are even longer. This justifies the use of the nonradiative self-similar solution.

Another effect that can change the structure is the efficient acceleration of relativistic particles. If relativistic particles are an important contributor to the pressure, the adiabatic index approaches  $4/3$  and the compression ratio in the shock front is increased. The result is a decrease in the width of the shocked region (Chevalier 1983). If there are losses of relativistic particles from the shocked region, the compression in the shocked region is increased further (e.g., Ellison & Reynolds 1991).

#### 4. RELATIVISTIC PARTICLE SPECTRUM

Particle acceleration is most likely to occur at the shock fronts resulting from the interaction. There are reasons to believe that the forward shock dominates the reverse shock in contributing to the relativistic particle component. The forward shock has a higher velocity, postshock energy density, and volume of shocked gas. In addition, the preshock magnetic field at the reverse shock is small because of the expansion of the supernova. In the case of

Tycho’s supernova remnant, Warren et al. (2005) have argued on the basis of X-ray observations that the particle acceleration is primarily at the forward shock and not at the reverse shock.

Loss processes that can affect the particle distribution are synchrotron losses and inverse Compton losses. We assume that a fraction  $\epsilon_B$  of  $\rho_0 v_s^2$ , where  $\rho_0$  is the preshock circumstellar density and  $v_s$  is the forward shock velocity, is converted to magnetic energy density,  $u_B$ , so that

$$u_B = 0.052 \epsilon_{B-1} A_* t_{10}^{-2} \text{ erg cm}^{-3}, \quad (8)$$

where  $\epsilon_{B-1}$  is  $\epsilon_B/0.1$  and  $t_{10}$  is the age in units of 10 days. The value of  $B$  for the reference parameters is 1.1 G. Assuming that electrons radiate at their critical synchrotron frequency, the Lorentz factor of electrons radiating at frequency  $\nu$  is

$$\gamma = 56 \nu_{10}^{0.5} \epsilon_{B-1}^{-0.25} A_*^{-0.25} t_{10}^{0.5}, \quad (9)$$

where  $\nu_{10} = \nu/10^{10}$  GHz. The synchrotron cooling time can then be written as

$$t_{syn} = 14 \nu_{10}^{-0.5} \epsilon_{B-1}^{-0.75} A_*^{-0.75} t_{10}^{1.5} \text{ day} \quad (10)$$

and the critical frequency at which the synchrotron cooling time equals the age is

$$\nu_{c10} = 1.8 \times 10^2 \epsilon_{B-1}^{-1.5} A_*^{-1.5} t_{10}. \quad (11)$$

It can be seen that synchrotron cooling is typically not important when considering radio emission, but is important when considering X-ray emission. If the electron shock acceleration extends to a high energy, the effect of synchrotron cooling is to steepen the energy spectrum from  $p$  to  $p + 1$ .

As discussed by Björnsson & Fransson (2004), inverse Compton losses can be significant when considering the radio emission from a Type Ic supernova. The radiation field is dominated by that from the supernova photosphere, which gives an energy density  $u_{rad} = L/(4\pi R^2 c)$ , where  $L$  is the supernova luminosity. Consideration of the light curve shape for a SN Ib/c shows that the Compton cooling is most important close to maximum light. For events like SN 1994I and SN 2002ap, the luminosity peaked at  $\sim 2 \times 10^{42}$  erg s $^{-1}$ , when the age was 10 days. The Compton cooling time can be written as

$$t_C = \frac{25.2}{u_{rad} E} = 16 \nu_{10}^{-0.5} \epsilon_{B-1}^{0.25} A_*^{0.01} t_{10}^{1.26} E_{51}^{0.88} M_1^{-0.64} \left( \frac{L}{2 \times 10^{42} \text{ erg s}^{-1}} \right)^{-1} \text{ day}, \quad (12)$$

where cgs units are used in the first expression. This result shows that Compton cooling can have some effect near maximum light, as was found by Björnsson & Fransson (2004) for SN 2002ap, but that it is probably not important at later times.

From equations (10) and (12), the ratio of synchrotron cooling time to inverse Compton cooling time is

$$\frac{t_{syn}}{t_{IC}} = 0.9\epsilon_{B-1}^{-1.0}A_*^{-0.76}t_{10}^{0.24}E_{51}^{-0.88}M_1^{0.64} \left( \frac{L}{2 \times 10^{42} \text{ erg s}^{-1}} \right). \quad (13)$$

After maximum light, the luminosity  $L$  drops more rapidly than  $t^{-0.24}$ , so synchrotron cooling is expected to be the dominant cooling process.

Assuming that the maximum energy to which electrons are accelerated,  $E_{max}$ , is limited by synchrotron losses, we have (e.g., Reynolds 1998)

$$E_{max} \propto B^{-1/2}v_s G^{1/2}, \quad (14)$$

where  $v_s$  is the forward shock velocity, and  $G$  is a factor to account for inverse Compton losses and is  $\propto u_B/u_{rad}$  when the inverse Compton losses dominate the synchrotron losses. The constant of proportionality in equation (14) depend on details of the shock acceleration process and the obliquity of the shock front. Taking the synchrotron emission to be at the critical frequency, the maximum frequency for the synchrotron emission is

$$\nu_{max} \propto BE^2 \propto v_s^2 G. \quad (15)$$

X-ray synchrotron emission has been observed from Galactic supernova remnants like SN 1006 with  $v_s \approx 3000 \text{ km s}^{-1}$  (Koyama et al. 1995), so the high velocities present in young supernovae should produce emission beyond the X-ray regime if synchrotron losses dominate. The above considerations show that synchrotron losses typically do dominate, except near maximum optical light when  $G \sim 0.1$  for the standard parameters. Even in this case, the emission should extend to X-ray wavelengths. The synchrotron cooling time is much less than the age at these high frequencies, so the supernova age is not a limiting factor in determining the maximum particle energy.

As noted in § 2, radio observations of SNe Ib/c indicate an energy spectral index  $p \approx 3$  over a broad range of times. The fact that synchrotron and inverse Compton losses are unlikely to affect the spectrum implies that this is the injection spectrum for the radiating particles. Diffusive shock acceleration in the test particle limit is well known to give the result  $p = (r + 2)/(r - 1)$ , where  $r$  is the shock compression. A nonrelativistic shock with  $r = 4$  gives  $p = 2$ . A steeper spectrum is possible if there is feedback to the acceleration process and the lower energy particles cross a subshock with a relatively low degree of compression (e.g., Ellison & Reynolds 1991; Ellison et al. 2000). Higher energy particles experience a higher degree of compression and thus have a flatter spectrum; there is the possibility of curvature in the spectrum. The total compression can be  $r > 4$  (leading to  $p < 2$ ) because

of the relativistic contribution to the equation of state and the loss of high energy particles from the shock region.

At the high shock velocities in SNe Ib/c, many of the postshock electrons can be accelerated to relativistic velocities. If a fraction  $\epsilon_{et}$  of the total postshock energy density goes into electrons then (cf. Soderberg et al. 2005)

$$\epsilon_{et} \left( \frac{v}{c} \right)^2 \frac{m_p c^2}{r} \approx \bar{\gamma} m_e c^2, \quad (16)$$

where  $\bar{\gamma}$  is the average Lorentz factor of the postshock electrons. The electron distribution behind fast shocks is not well understood theoretically. In the field of GRBs, it is commonly assumed that all the electrons go into a power law spectrum with energy index  $p$ , above some Lorentz factor  $\gamma_{min}$ . If a similar assumption is made here, then

$$\bar{\gamma} = (p - 1)\gamma_{min}/(p - 2); \quad (17)$$

in this case  $\epsilon_e = \epsilon_{et}$ , where  $\epsilon_e$  is the fraction of the postshock energy density that goes into nonthermal relativistic electrons. The requirement that  $\gamma_{min} > 1$  gives

$$\epsilon_e > 0.16 \left( \frac{v_s}{50,000 \text{ km s}^{-1}} \right)^{-2} \quad (18)$$

for  $p = 3$  and we have assumed that low energy particles dominate the electron energy. The postshock energy is distributed among the electrons, magnetic field, and protons/ions, so  $\epsilon_e \lesssim 0.33$  is likely. If the constraint in equation (18) is not fulfilled, there is a significant nonrelativistic electron component.

## 5. RADIO EMISSION

The basic physical mechanisms relevant to the radio emission from SNe Ib/c have been discussed by Chevalier (1998) and Björnsson & Fransson (2004). There is an early phase when synchrotron self-absorption is important, followed by an optically thin decline. If these are the only significant processes and the injected power law particle spectrum does not vary, the radio light curves at various frequencies are self-similar. However, as discussed in Björnsson & Fransson (2004) and in § 4, the action of inverse Compton cooling near optical maximum light can depress the radio light curves in the optically thin phase.

An additional factor noted above is that there is a minimum Lorentz factor for the electrons,  $\gamma_{min}$ , and the radio emission is affected if electrons with this energy radiate in the radio. Combining equations (3), (16) and (17), we have

$$\gamma_{min} = 0.3\epsilon_{e-1}E_{51}^{0.88}M_1^{-0.64}A_*^{-0.24}t_{10}^{-0.24}, \quad (19)$$

which corresponds to a frequency

$$\nu_m = 0.5 \times 10^7 \epsilon_{e-1}^2 \epsilon_{B-1} E_{51}^{1.76} M_1^{-1.28} t_{10}^{-1.5} \text{ Hz.} \quad (20)$$

These equations are sensible only if the parameters yield  $\gamma_{min} > 1$ ; it can be seen that, in typical cases, not all the electrons are accelerated to a relativistic velocity. The frequency  $\nu_m$  is equivalent to the  $\nu_m$  used in studies of GRB afterglows. In the supernova case,  $\nu_m$  is typically below the observed radio wavelength region; a supernova with unusually high energy and low mass is needed to have an observable effect of  $\nu_m$ .

A more important effect is the normalization of the relativistic electron particle distribution function. Chevalier (1998) assumed that the power law distribution extends down to  $m_e c^2$  and the energy density in the relativistic component is proportional to the postshock energy density. In this case, if  $N(E) = N_0 E^{-p}$ , then  $N(E) \propto t^{-2}$  and  $L_\nu \propto R^3 N_0 B^{(p+1)/2} \propto t^{-(5+p-6m)/2}$ . In the case that  $\gamma_{min} > 1$ , the same assumption about the evolution of the energy density leads to  $N_0 \propto R^{2(p-2)} t^{-2(p-1)} \propto t^{2(m-1)(p-1)-2m}$ , and thus  $L_\nu \propto t^{(4mp-5p-2m+3)/2}$ . For the particular case  $p = 3$ , which is relevant to SNe Ib/c, we have  $L_\nu \propto t^{5m-6}$ , as opposed to  $t^{3m-4}$  for the standard case; the decline is steeper by  $t^{-2(1-m)}$ .

The model properties for the optically thin regime can be compared to the observed properties in Table 1. The spectral indices of  $\alpha \approx -1.0$  correspond to  $p \approx 3$ . Over the range of ages where the observations are made, we do not expect inverse Compton or synchrotron losses to be important for the radio emitting electrons (§ 4), implying that  $p \approx 3$  is the injection spectrum. As discussed in § 4, this is steeper than the result expected in the test particle limit ( $p = 2$ ) and may imply that the accelerating shock wave is cosmic ray dominated. One exception is SN 2002ap, which was observed at an early time near the peak optical luminosity when inverse Compton cooling may be important. Björnsson & Fransson (2004) have argued that in this case the particles are injected with  $p \approx 2$  and the spectrum is steepened to  $p \approx 3$  by inverse Compton losses. This model can explain the flatter rate of decline of the radio emission.

The observed spectral index is in approximate accord with expectations from the nonlinear shock theory. Ellison & Reynolds (1991, their Fig. 8) show that the expected spectral index is compatible with those observed in young Galactic supernova remnants for models in which electron acceleration occurs to high maximum energy. The electrons in radio supernovae radiate in a higher magnetic field, so their energies are lower,  $\gamma \sim 90$  (eq. [9]), and the energy index expected in the model is  $p \approx 2.8$ . Ellison et al. (2000, their Fig. 2) approximate the electron spectrum as power law segments with a break at  $\gamma \sim 10^3$ ; below the break,  $p \approx 2.8$ . Thus, there is approximate accord between the nonlinear shock model and the supernova observations. A prediction of this model is that the observed radio spectra should flatten with time. However, the evolution is slow. A factor of 10 increase in age

leads to an increase in  $\gamma$  by 3.2 (eq. [9]) and a flattening in  $p$  by  $\sim 0.1$  (Fig. 8 of Ellison & Reynolds 1991). This is not observable in currently available supernova radio light curves of SNe Ib/c.

The standard model for the optically thin decline, with  $m = 0.88$  and  $p = 3$ , gives  $\beta = -1.3$ . An uncertainty of  $\pm 0.3$  in  $p$  corresponds to  $\pm 0.15$  in  $\beta$ . If the lowest electron energy evolves with time, the decline steepens by 0.2. The observed range in  $\beta$  (Table 1) can be plausibly accounted for, although the mechanism that is primarily responsible for the range is not known. One discrepant decline is the relatively flat decline of SN 2002ap, which can be accounted for by the inverse Compton cooling model of Björnsson & Fransson (2004).

### 5.1. Range of Radio Luminosity

One of the most notable radio properties of SNe Ib/c is the large range of radio luminosity. This is exemplified by the fact that SN 2003L had a higher peak luminosity than SN 2002ap by  $\sim 10^3$ ; if one considered the luminosity at the same time during the optically thin phase ( $\sim 100$  day), the difference would be  $\sim 2 \times 10^4$ . Here we investigate possible reasons for the luminosity range of the supernovae.

We assume that the supernovae are characterized by the same value of  $m$ ; the possible variation in this quantity is small and we do not expect it to contribute to the luminosity difference. We also assume that the particle spectra are characterized by  $p = 3$ . If the relativistic electron spectrum extends to  $m_e c^2$ , the radius of the forward shock wave at the time of the synchrotron self-absorption peak is (Chevalier 1998)

$$R_p = 4.0 \times 10^{14} \alpha^{-1/19} \left( \frac{f}{0.5} \right)^{-1/19} \left( \frac{F_{op}}{\text{mJy}} \right)^{9/19} \left( \frac{D}{\text{Mpc}} \right)^{18/19} \left( \frac{\nu}{5 \text{ GHz}} \right)^{-1} \text{ cm}, \quad (21)$$

where  $\alpha = \epsilon_e / \epsilon_B$  is the ratio of relativistic electron energy density to magnetic energy density,  $f$  is the fraction of the spherical volume occupied by the radio emitting region,  $F_{op}$  is the observed peak flux, and  $D$  is the distance. The results for  $R_p / t_p$ , where  $t_p$  is the age at peak flux, are given in Table 3, and can be compared to expectations from the hydrodynamic model (eq.[3]). The model shows agreement with the observations for plausible supernova parameters; the radio emission can be attributed to the shock region generated by the outer supernova ejecta.

Once  $R_p / t_p$  is determined, the forward shock velocity can be found from  $v_s \approx 0.88 R_p / t_p$ , and  $\gamma_{min}$  from equations (16) and (17). The electron spectra extend to the nonrelativistic range, as assumed in equation (21), except for SN 2002ap, for which  $\gamma_{min} = 2.2$  if  $\epsilon_e = 0.1$ .

We have  $R_p \propto \gamma_{min}^{-(p-2)/(2p+13)} \propto \gamma_{min}^{-1/19}$  ( $p = 3$ ) (Chevalier 1998), resulting in  $R_p$  being reduced by 0.96 for SN 2002ap. The effect on the velocity is small.

The magnetic field at the time of the synchrotron self-absorption peak is (Chevalier 1998)

$$B_p = 1.1 \alpha^{-4/19} \left( \frac{f}{0.5} \right)^{-4/19} \left( \frac{F_{op}}{\text{mJy}} \right)^{-2/19} \left( \frac{D}{\text{Mpc}} \right)^{-4/19} \left( \frac{\nu}{5 \text{ GHz}} \right) \text{ G}, \quad (22)$$

where  $f$  is the fraction of the spherical volume occupied by the radio emitting region and  $F_{op}$  is the observed peak flux. This expression again assumes that the electron energy distribution extends down to  $\sim m_e c^2$ . For SN 2002ap, the fact that  $\gamma_{min} > 1$  leads to a higher value of  $B_p$  by a factor of 1.17.

Combining this  $B$  field estimate with equation (8) leads to

$$A_* \epsilon_{B-1} \alpha^{8/19} = 1.0 \left( \frac{f}{0.5} \right)^{-8/19} \left( \frac{F_{op}}{\text{mJy}} \right)^{-4/19} \left( \frac{D}{\text{Mpc}} \right)^{-8/19} \left( \frac{\nu}{5 \text{ GHz}} \right)^2 t_{10}^2. \quad (23)$$

The results for the observed supernovae are in Table 3. SN 2003L stands out as having a high circumstellar density:

$$A_* = 35 \epsilon_{B-1}^{-1} \alpha^{-8/19} = 35 \left( \frac{\epsilon_e}{0.1} \right)^{-8/19} \left( \frac{\epsilon_B}{0.1} \right)^{-11/19}. \quad (24)$$

The maximum value for the  $\epsilon$ 's is  $\sim 1/3$ , so the implication is that the circumstellar density around SN 2003L is high for a Wolf-Rayet star and may require special circumstances at the end of the star's evolution. This is consistent with the fact that SNe Ib/c are rarely as radio luminous as SN 2003L (Berger et al. 2003; Soderberg et al. 2006a).

If we make the assumption that the difference in radio properties is due to differences in circumstellar density ( $A_*$ ) and that the supernovae are similar, the velocity difference between SN 2002ap and SN 2003L can be compared to that expected in the hydrodynamic model,  $R_p/t_p \propto A_*^{-0.12} t_p^{-0.12}$  (eq. [3]). The predicted velocity ratio is 3.2, whereas the observed is 3.3; the high velocity in SN 2002ap can be attributed to the low circumstellar density and early time of observation. However, differences in the supernovae could also contribute to the differences in velocity. For SN 2002ap, Mazzali et al. (2002) have estimated an explosion energy of  $(4 - 10) \times 10^{51}$  ergs and ejecta mass of  $2.5 - 5 M_\odot$ , although these values are quite uncertain. Estimates for SN 2003L are not available.

Overall, the range in the radio luminosities of SNe Ib/c can be accounted for by the expected range in the circumstellar densities, as deduced from the range of circumstellar densities in Galactic Wolf-Rayet stars, if  $\epsilon_B \sim 0.1$ . However, some contribution to the range from variations in the  $\epsilon$  efficiency parameters cannot be ruled out and may be needed to give

the broad distribution of peak luminosities of the SNe Ib/c. As argued in Chevalier (1998), the high magnetic fields found in SNe Ib/c cannot plausibly be attributed to the shock compression of the ambient stellar wind magnetic field and field amplification is required. One mechanism for field amplification is the turbulence generated by hydrodynamic instabilities in the decelerating shocked shell. However, Jun & Norman (1996) find that  $u_B$  generated in this way is  $< 1\%$  of the turbulent energy density, although this result may be an underestimate due to the finite numerical resolution. An alternative mechanism for amplification is the turbulence generated by the diffusive shock acceleration of cosmic rays. Bell (2004) finds that this mechanism can generate a magnetic energy density  $u_B \sim (1/2)(v_s/c)u_{cr}$ , where  $u_{cr}$  is the cosmic ray energy density. Because we expect that  $u_{cr}$  is a large part of the postshock energy density, efficient field amplification can be accomplished because  $v_s/c \sim 0.1$  for SNe Ib/c. An implication of this scenario is that  $\epsilon_B$  is not constant, as we have assumed, because of the evolution of  $v_s$ . However, the evolution is modest,  $v_s \propto t^{-0.12}$ . The effect on the optically thin flux evolution is likewise modest because  $F_\nu \propto B^{(p+1)/2} \propto B^2$  for  $p = 3$ . The steepening of the flux evolution is by  $t^{-0.12}$ .

## 6. X-RAY EMISSION

Since the first X-ray observations of supernovae, three mechanisms have been discussed for the emission: synchrotron radiation, thermal emission, and inverse Compton emission (Canizares, Kriss, & Feigelson 1982; Chevalier 1982b; Fransson 1982), and they are the mechanisms that we discuss here. The results deduced from the radio emission provide a starting point for the physical conditions that can be expected. However, the radio observations do not provide a unique model; the combination of radio and X-ray data can be expected to better define the physical situation in the SNe Ib/c.

### 6.1. Thermal Emission

For a given set of parameters  $M$ ,  $E$ , and  $A$ , the hydrodynamic interaction is well-defined, and the density and pressure profiles are determined. Thermal emission is dominated by emission from the reverse shock region. If the postshock gas is in ionization and temperature equilibrium, the temperature is

$$T_{eq} = 5.7 \times 10^8 \zeta_1 E_{51}^{0.88} \left( \frac{M}{10 M_\odot} \right)^{-0.64} A_*^{-0.24} t_d^{-0.24} \text{ K}, \quad (25)$$

where the gas is assumed to be fully ionized, and  $\zeta_1 = 1/2$  for H and  $2Z/(Z+1)$  for heavy elements with charge  $Z$ .

The time scale for energy transfer from ions to electrons is

$$t_{e-i} = \frac{4.2 \times 10^{-22}}{\ln \Lambda} \zeta_2(Z) \frac{T_e^{3/2}}{\rho}, \quad (26)$$

where  $\zeta_2 = 1$  for H and  $\zeta_2 = 4/Z$  for heavier elements of charge  $Z$  and  $\ln \Lambda \approx 30$  is the Coulomb logarithm. For the reverse shock this can be written as

$$t_{e-i} = 51 \zeta_2(Z) \left( \frac{v_s}{5 \times 10^4 \text{ km s}^{-1}} \right)^2 \left( \frac{T_e}{10^8 \text{ K}} \right)^{3/2} A_*^{-1} t_{10}^2 \text{ days.} \quad (27)$$

The reverse shock temperature is  $\gtrsim 5 \times 10^8$  K and it is clear that the electrons and ions can not be kept in equipartition by Coulomb collisions only. We can reverse this and estimate the minimum electron temperature:

$$T_e = 3.2 \times 10^7 \zeta_2(Z)^{-2/3} \left( \frac{v_s}{5 \times 10^4 \text{ km s}^{-1}} \right)^{-4/3} A_*^{2/3} t_{10}^{-2/3} \text{ K.} \quad (28)$$

For an oxygen dominated ejecta, the typical temperature is  $(0.5 - 2) \times 10^8$  K; a helium dominated composition will give a temperature lower by a factor  $\sim 2.5$ . It is plausible that plasma instabilities in the shock lead to a higher value, as is the case for supernova remnants. Complete equipartition is, however, unlikely.

We have also estimated the timescale for collisional ionization behind the reverse shock, which can be written

$$t_{ion} = \frac{1.2 \times 10^{-11}}{C_i(T_e)} \left( \frac{v_s}{5 \times 10^4 \text{ km s}^{-1}} \right)^2 A_*^{-1} t_{10}^2 \text{ days,} \quad (29)$$

where  $C_i(T_e)$  is the collisional ionization rate for ion  $i$ , and we have assumed a composition dominated by helium or heavier elements. Assuming a temperature given by the pure Coulomb heating case we find that, although the timescale is strongly dependent on the composition, intermediate mass elements like oxygen will in general be completely ionized, while heavy elements like iron will be in their He-like stages, i.e. under-ionized with respect to the temperature. For the Type Ic SN 1994I, Iwamoto et al. (1994) propose an outer layer with a composition X(O)=0.43, X(C)=0.45, and X(He)=0.09. On the other hand, SNe Ib have He lines in their optical spectra, and Branch et al. (2002) find that there is typically evidence for H in the highest velocity layers. The expected composition should lead to complete ionization.

If the gas is completely ionized, the free-free emission from the reverse shocked gas can be estimated (Chevalier & Fransson 2003)

$$L_{ff} = 3 \times 10^{35} \frac{(n-3)(n-4)^2}{4(n-2)} \beta^{1/2} \zeta_2^{-1} A_*^2 t_{10}^{-1} \text{ erg s}^{-1} = 2.4 \times 10^{36} \beta^{1/2} \zeta_2^{-1} A_*^2 t_{10}^{-1} \text{ erg s}^{-1}, \quad (30)$$

where  $\beta = T_e/T_{eq}$  and the second expression is for  $n = 10$ . Over the timescales of interest for the X-ray observations, circumstellar X-ray absorption is expected to be negligible for SNe Ib/c.

Substitution of the values of  $A_*$  from Table 3 shows that the predicted thermal X-ray luminosity falls below the observed luminosity by orders of magnitude in every case. Immler, Wilson, & Terashima (2002) discussed a thermal interpretation of the X-ray emission from SN 1994I, but they required  $\dot{M} = 10^{-5} M_\odot \text{ yr}^{-1}$  for an assumed  $v_w = 10 \text{ km s}^{-1}$ , or  $A_* = 100$ . This can be compared to  $\epsilon_{B-1}A_* \approx 2.7$  deduced here. Although a low value of  $\epsilon_{B-1}$  could bring up  $A_*$  to the required value, the mass loss rate would be considerably higher than that expected for a Wolf-Rayet star. In view of this, we explore nonthermal mechanisms for the X-ray emission.

## 6.2. Inverse Compton X-Ray Emission

One type of inverse Compton emission is scattering of photospheric photons with thermal hot electrons in the shock interaction region (Fransson 1982). Sutaria et al. (2003) suggested that this mechanism is responsible for the X-ray emission observed from SN 2002ap. However, the required electron optical depth and position of the hot electrons are not compatible with the hydrodynamic situation expected in SN 2002ap, and inverse Compton scattering of photospheric photons by relativistic electrons is more plausible (Björnsson & Fransson 2004). The observed radio emission from a supernova gives information on the spectrum of relativistic electrons.

The radio observations of SNe Ib/c show that the power law electron spectrum is well approximated by  $p = 3$ . For this case, the inverse Compton X-ray luminosity is (Chevalier, Fransson, & Nymark 2006)

$$\frac{dL_{\text{IC}}}{dE} \approx 8.8 \times 10^{36} \epsilon_{r-1} \gamma_{\min} E_{\text{keV}}^{-1} A_* v_{s4} \left( \frac{L_{\text{bol}}(t)}{10^{42} \text{ erg s}^{-1}} \right) t_{10}^{-1} \text{ ergs s}^{-1} \text{ keV}^{-1}, \quad (31)$$

where  $\gamma_{\min}$  is the minimum Lorentz factor of the relativistic electrons,  $v_{s4}$  is the forward shock velocity in units of  $10^4 \text{ km s}^{-1}$ , and  $L_{\text{bol}}$  is the bolometric luminosity of the supernova. Instead of  $A_*$ , the radio emission gives the quantity  $S_* \equiv \epsilon_{B-1} A_* \alpha^{8/19}$ , so that equation (31) becomes

$$E \frac{dL_{\text{IC}}}{dE} \approx 8.8 \times 10^{36} \gamma_{\min} S_* \alpha^{11/19} v_{s4} \left( \frac{L_{\text{bol}}(t)}{10^{42} \text{ erg s}^{-1}} \right) t_{10}^{-1} \text{ ergs s}^{-1}. \quad (32)$$

The epsilon parameters now enter only through the ratio  $\alpha = \epsilon_e/\epsilon_B$ .

Predictions of the X-ray luminosity using equation (32) are given in Table 4, where

the values of  $v_s$  have been taken from the velocity at peak radio luminosity (Table 3) and evolved to the time of the X-ray observation. The value of  $\alpha$  is assumed to be 1. The values of  $L_{bol}$  for SN 2002ap, 2003L, and 2003bg are given in the references listed in Table 3. The early values for SN 1994I are from Richmond et al. (1996). No direct optical observations of SN 1994I at an age of 7 years are available, but estimates of the luminosity are possible by analogy to SN 1987A. At an age of 7 years, SN 1987A had faded by 15 magnitudes from maximum light (Suntzeff 2003), to  $\sim 2 \times 10^{36}$  erg s $^{-1}$ . The power input is presumably from  $^{44}\text{Ti}$  at this age and SNe Ib/c are estimated to have  $\lesssim 10^{-4} M_\odot$  of  $^{44}\text{Ti}$  synthesized in the explosion (Timmes et al. 1996), comparable to the  $\sim 10^{-4} M_\odot$  of  $^{44}\text{Ti}$  estimated for SN 1987A. In addition, the estimated mass of  $^{56}\text{Ni}$ ,  $0.07 M_\odot$  (Young, Baron, & Branch 1995), is comparable to that ejected in SN 1987A. The late luminosity of SN 1994I, is probably considerably less than  $2 \times 10^{36}$  erg s $^{-1}$  because the ejected mass in SN 1994I,  $\sim 1 M_\odot$  (Young, Baron, & Branch 1995), is much less than that of SN 1987A and the ejecta are less able to absorb the radioactive power. There is not a published optical light curve for SN 2001ig, so we used amateur photometric measures (Pelle 2004) to estimate the bolometric luminosity for this case.

The results show varying degrees of agreement with the observed X-ray luminosities. The observation that is most consistent with the expectations from inverse Compton is the early observation of SN 2002ap, which is in agreement with the interpretation of Björnsson & Fransson (2004). The other predictions of inverse Compton emission are lower than expected, and require high values of  $\alpha = \epsilon_e/\epsilon_B$  to come into agreement with the observed luminosities. A problem with departures from energy equipartition of magnetic fields and electrons ( $\alpha \neq 1$ ) is that we argued for  $\epsilon_e \approx \epsilon_B \approx 0.1$  in order to approximately reproduce the range of Wolf-Rayet wind densities. Because the  $\epsilon$ 's are expected to be  $\lesssim 1/3$ , the possible departure from equipartition is limited; this argument especially applies to the radio luminous supernovae (SN 2003L and SN 2003bg).

A general expectation of the inverse Compton model is the relation between the optical luminosity and the inverse Compton luminosity (eq. [32]); this relation is not shared by other mechanisms (thermal and synchrotron). The existing X-ray observations do not provide good light curve coverage, but, where multiple epochs do exist, they do not show the expected relation. The large decline expected between days 30 and 120 for SN 2003bg does not appear in the observed fluxes, which argues against the inverse Compton mechanism, at least at the late time. For SN 1994I, the inverse Compton definitely fails to explain the late time observations, as will be shown explicitly in §6.3. Searches for inverse Compton emission should concentrate on observations around the time of maximum optical light.

### 6.3. Synchrotron

Because of the lack of a detailed theory for the acceleration of relativistic electrons, the X-ray synchrotron emission is typically estimated by extending the radio synchrotron emission into the X-ray regime. In view of the relatively steep spectra of SNe Ib/c and further steepening expected from synchrotron losses, a simple extrapolation of the optically thin radio emission leads to a low X-ray luminosity. Table 2 gives the value of  $\nu L_\nu$  for the various supernovae at 5 GHz; in cases where there are no radio observations at the time of the X-ray observations or the emission is optically thick at 5 GHz, a rough extrapolation of the radio evolution has been made. With  $L_\nu \propto \nu^{-1}$ , as is approximately observed in these supernovae, the quantity  $\nu L_\nu$  stays constant with frequency. It can be seen that the X-ray luminosity is above this extrapolation (Table 4); if synchrotron losses to the electron spectrum were included, the discrepancy would be larger. It is for this reason that the synchrotron mechanism is generally not found to be viable for X-ray supernovae (e.g., Soderberg et al. 2005, on SN 2003L).

However, as described in § 4, the nonlinear theory of particle acceleration predicts that the electron spectrum becomes flatter for  $\gamma \gtrsim 10^3$ . We use an approximate version of this theory to estimate whether synchrotron emission can account for the late emission from SN 1994I. Following Ellison et al. (2000), we assume power law segments for the electron energy distribution. Below  $\gamma = 10^3$ , we take  $p = 3$ , and for  $\gamma > 10^3$ ,  $p = 2$ . This injection spectrum for the particles extends to X-ray emitting particles, as argued above. The frequency corresponding to the spectral break is  $\nu_{br} = 3.4 \times 10^{12} B$  Hz. For the situation here, we have  $B \propto t^{-1}$ , which also gives the time dependence of  $\nu_{br}$ . For the magnetic field estimated in SN 1994I (Table 3),  $\nu_{br} = 6.5 \times 10^{12} t_{10}^{-1}$  Hz.

The injection spectrum is modified by inverse Compton and synchrotron losses; at the late times of interest here, synchrotron losses are expected to be the dominant mechanism. The frequency at which synchrotron losses become important,  $\nu_c$ , can be found from equation (10). For the magnetic field estimated for SN 1994I, we have  $\nu_c = 4.1 \times 10^{11} t_{10}$  Hz. For these conditions,  $\nu_c > \nu_{br}$  provided that  $t > 40$  days. At the times of interest, the particle spectrum steepens to  $p = 3$  for  $\nu > \nu_c$ . We then have

$$\frac{\nu L_{\nu, X-ray}}{\nu L_{\nu, radio}} = \left( \frac{\nu_c}{\nu_{br}} \right)^{1/2} \propto t. \quad (33)$$

For the parameters relevant to SN 1994I at an age of 2500 days,  $\nu L_{\nu, X-ray}/\nu L_{\nu, radio} = 62$ . The synchrotron mechanism is thus able to approximately account for the late X-ray emission from SN 1994I in the context of a particle spectrum formed in a cosmic ray dominated shock. Equation (33) shows that, with the synchrotron mechanism, the evolution of  $L_{X-ray}$  is flatter

than  $L_{radio}$  by one power of  $t$ . For the radio evolution observed for SN 1994I (Table 1), the predicted evolution is  $L_{X-ray} \propto t^{-0.3}$ .

Although this gives an estimate of the expected emission, we have carried out more detailed calculations of the effects of synchrotron and inverse Compton radiation on the particle spectrum and emission, using the methods of Fransson & Björnsson (1998). One calculation was to assume a particle injection spectrum with  $p = 3.1$ , normalized to reproduce the radio emission from SN 1994I, and a bolometric supernova optical light curve like that of SN 1994I, taken from Richmond et al. (1996). The optical emission is important for inverse Compton effects. We assume  $\epsilon_e = \epsilon_B = 0.1$ ,  $A_* = 3$ ,  $v_s(t) = 6 \times 10^4(t/10 \text{ days})^{-1/8} \text{ km s}^{-1}$  (i.e.,  $n = 10$ ). This model fails to reproduce the late X-ray emission from SN 1994I by a large factor (Fig. 1). In another model, we include an injection spectrum appropriate to a cosmic ray dominated shock wave, as calculated by Ellison et al. (2000, their Fig. 1). The flattening of the spectrum to high energy greatly enhances the X-ray synchrotron emission (Fig. 1), while the effect on the radio emission is minor. Finally, we show this same calculation, but with a supernova light curve appropriate to SN 1997ef, which had a broader optical maximum than SN 1994I (Iwamoto et al. 2000). The effect on the inverse Compton X-ray emission near maximum light can be seen (Fig. 1), and it is clear that inverse Compton emission is important only during the first  $\sim 50$  days even for a broad optical light curve such as SN 1997ef. These results confirm that the cosmic ray dominated shock model can explain the observed X-ray emission on day  $\sim 2500$ . The model is also consistent with the observed upper limit on day 52, but falls below the detection on day 82. However, the early detection of SN 1994I did not have high statistical significance:  $3.4\sigma$  in a 6.4 ks observation and  $3.1\sigma$  in a 29.9 ks observation with ROSAT (Immler, Pietsch, & Aschenbach 1998).

Fig. 1 shows that the X-ray light curves have an imprint of the optical light curve due to inverse Compton radiation near maximum light. Selected spectra show the basic components of the multiwavelength spectrum: optical photospheric emission, inverse Compton emission, and synchrotron radiation (Fig. 2). At 10 days there is a strong inverse Compton component extending from the ultraviolet to the X-rays. At 30 days this has almost disappeared. The curvature of the synchrotron component is apparent, especially at 10 days when the radio range is also affected by cooling. For SN 1994I, we cannot rule out the possibility of late dense circumstellar interaction giving rise to thermal X-ray emission because there are not simultaneous observations at other wavelengths. In our model, this would require dense matter at some distance from the supernova, as appears to be the case in SN 2001em (Chugai & Chevalier 2006). Our suggestion of late synchrotron emission from a Type Ic like SN 1994I needs confirmation from more complete X-ray observations of a similar event. Spectral observations would provide the most direct constraints, but as Fig. 1 shows, the evolution of the X-ray light curve can also discriminate between different mechanisms.

#### 6.4. SN 1998bw

None of the supernovae discussed so far have a clear connection with GRBs and the emission can be accounted for by an interaction region driven by the fast outer supernova ejecta. SN 1998bw was observed as a bright SN Ic and was associated with GRB 980425. The early turn-on of the radio emission suggests mildly relativistic expansion in the synchrotron self-absorption model (Kulkarni et al. 1998; Li & Chevalier 1999); this implies that the nonrelativistic analysis presented here may not be accurate, but it can still be expected to give approximate results. The early peak emission (42 mJy 5 GHz flux at 13 days) implies  $\epsilon_{B-1} A_* \approx 0.1$ . For a comparable efficiency of magnetic field production, the circumstellar density is low for SN 1998bw compared to the typical SN Ib/c.

SN 1998bw has been observed as an X-ray source over days 1 – 1200, showing a remarkably low rate of decline (Kouveliotou et al. 2004) (a factor  $\sim 10$  over this time period). Inverse Compton scattering of photospheric photons would decline much more rapidly after maximum light, so synchrotron emission is the most likely emission mechanism. The radio emission has an optically thin spectral index  $\nu^{-0.75}$ , implying  $p \approx 2.5$ . If the observed flux at  $t = 100$  days is extended to the X-ray range, the luminosity falls short of the observed X-ray luminosity by a factor of  $\sim 10$ . Considering that synchrotron losses can further decrease the X-ray flux by 20, the radio through X-ray emission is not consistent with injection of electrons with a single power law index. As discussed above, there are reasons to believe that the energy index might flatten at high energy if the shock waves are cosmic ray dominated. In this case, the synchrotron X-ray emission can decline more slowly than the radio emission (Fig. 1), as is observed in SN 1998bw. Alternatively, the X-ray emission could originate from a different region from the radio. Kouveliotou et al. (2004) discuss the possibility that the X-ray emission is related to off-axis emission from a fast jet related to the gamma-ray burst.

### 7. DISCUSSION AND CONCLUSIONS

We have found that the radio and X-ray emission from SNe Ib/c can be accounted for by supernova interaction with the wind from the Wolf-Rayet star progenitor. Following the arguments of Chevalier (1998), synchrotron self-absorption is generally responsible for the early absorption of the radio emission. The radio synchrotron emission from most of the SNe Ib/c considered here imply an electron energy index  $p \approx 3$ . The radio spectral index of SN 1998bw is distinctly flatter, with  $p \approx 2.5$ . The only other SN Ib/c with a relatively flat spectrum is SN 2002ap, with  $p \approx 2$  in the model of Björnsson & Fransson (2004). Interestingly, SN 2002ap has the highest velocity of any of the supernova in our group of

normal Ib/c events. It may be that as the shock velocity increases and relativistic effects become important, there are changes in the character of the particle acceleration.

The SNe Ib/c provide the opportunity to examine particle acceleration at shock velocities ( $\sim 0.1c$ ) intermediate between those present in Galactic supernova remnants and those in GRBs. Although the properties of the synchrotron radio emitting particles are clear ( $p \approx 3$  is typical), the properties of the X-ray synchrotron emission are uncertain. If the circumstellar densities are typical of Wolf-Rayet stars, thermal radiation cannot explain the observed X-ray emission and a nonthermal mechanism is required. Although inverse Compton scattering of photospheric photons might be able to explain X-ray emission close to maximum optical light, it generally fails to explain late emission. If this emission is synchrotron radiation, there must be a flattening of the particle spectrum at high energy, as can occur in diffusive acceleration in cosmic ray dominated shock waves. More detailed X-ray observations are needed to confirm this picture. We expect the early X-ray luminosity to be related to the optical luminosity of the supernova if it is inverse Compton emission; as the supernova fades, synchrotron emission may become the dominant mechanism, with a relatively slow rate of decline.

An additional piece of information from our interpretation is the magnetic field in the shocked region. If the circumstellar densities are typical of Wolf-Rayet stars, we find that efficient amplification of magnetic fields is needed, with  $\epsilon_B \sim 0.1$ . A possible reason for the field is a streaming instability that accompanies cosmic ray acceleration (Bell 2004), which may explain the high amplification at the high shock velocities present in SNe Ib/c. With this mechanism,  $\epsilon_B \propto v_s$ , so the value of  $\epsilon_B$  would be smaller in Galactic supernova remnants, as is observed.

This research was partially carried out while the authors were visiting the Kavli Institute of Theoretical Physics, supported in part by the National Science Foundation under Grant No. PHY99-07949. In addition, this research was supported in part by Chandra grant TM4-5003X and NSF grant AST-0307366 and the Swedish Research Council and Swedish National Space Board.

Table 1. Optically Thin Radio Properties of Type Ib/c Supernovae

Supernova	$\alpha$	$\beta$	Age (days)	References
1983N	-1.0	-1.6	30 – 300	1
1984L	-1.0	-1.5	100 – 200	2
1990B	-1.1	-1.3	70 – 200	3
1994I	-1.0	-1.3	20 – 800	4
2001ig	-1.06	-1.5	70 – 700	5
2002ap	-0.9	-0.9	4 – 20	6
2003L	-1.1	-1.2	100 – 400	7
2003bg	-1.1	-2	60 – 1000	8

The references to the data are: (1) Weiler et al. 1986; (2) Panagia et al. 1986; (3) Van Dyk et al. 1993; (4) Stockdale et al. 2005; (5) Ryder et al. 2004; (6) Berger et al. 2002; (7) Soderberg et al. 2005; (8) Soderberg et al. 2006b

Table 2. X-ray Observations of Type Ic Supernovae

Supernova	Distance (Mpc)	Age (days)	Luminosity ( $10^{38}$ ergs s $^{-1}$ )	$\nu L_\nu$ (5 GHz) ( $10^{38}$ ergs s $^{-1}$ )	References
1994I	8.3	52,82	< 1, 1.7 (0.3–2 keV)	0.04	1,2
”		2271,2637	0.17,0.14 (0.3–2 keV)	0.001	2
2001ig	12.3	170,191	1,0.6 (0.2–10 keV)	0.1	3,4
2002ap	10.4	4	0.9 (0.3–10 keV)	0.003	5,6
2003L	96	40	90 (2–10 keV)	13	7,8
2003bg	19.5	30,120	44,9 (0.3–10 keV)	7,3	9,10

The references to the data are: (1) Immler et al. 1998; (2) Immler et al. 2002; (3) Schlegel & Ryder 2002; (4) Ryder et al. 2004; (5) Rodriguez Pascual et al. 2002; (6) Sutaria et al. 2003; (7) Kulkarni & Fox 2003; (8) Soderberg et al. 2005; (9) Pooley & Lewin 2003; (10) Soderberg et al. 2006b

Table 3. Properties of Type Ib/c Supernovae in a Synchrotron Self-Absorption Model

Supernova	$t_p$ (days)	$\nu_p$ (GHz)	$F_{op}$ (mJy)	$D$ (Mpc)	$B_p$ G	$\epsilon_{B-1} A_* \alpha^{8/19}$	$R_p/t_p$ (km s $^{-1}$ )
1983N	21	4.88	18	5.1	0.56	1.15	42000
1990B	91	1.49	1.6	18.0	0.17	2.0	33000
1994I	36	4.86	17	8.3	0.51	2.8	38000
2001ig	42	4.8	18	12.3	0.46	3.1	49000
2002ap	8	1.43	0.3	10.4	0.26	0.04	105000
2003L	170	4.9	2.4	96	0.38	34	32000
2003bg	60	8.46	40	19.5	0.68	13	44000

Table 4. Expectations for Inverse Compton X-ray Luminosity

Supernova	Age (days)	$L_{bol}$ ( $10^{42}$ ergs s $^{-1}$ )	$v_s$ ( $10^4$ km s $^{-1}$ )	$\gamma_{min}$	$EdL_{IC}/dE$ ( $10^{38}$ ergs s $^{-1}$ )	$L_{obs}$ ( $10^{38}$ ergs s $^{-1}$ )
1994I	52	0.2	3.2	1	0.03	< 1
1994I	82	0.1	3.0	1	0.009	1.7
1994I	2271	2(-6)	2.0	1	4(-9)	0.17
1994I	2637	2(-6)	2.0	1	4(-9)	0.14
2001ig	170	0.15	3.6	1	0.009	1
2001ig	191	0.1	3.6	1	0.005	0.6
2002ap	4	1.5	10.0	2.5	0.2	0.9
2003L	40	1.6	3.3	1	4	90
2003bg	30	2.3	4.2	1	4	44
2003bg	120	0.3	3.6	1	0.1	9

## REFERENCES

Bell, A. R. 2004, MNRAS, 353, 550

Berger, E., Kulkarni, S. R., & Chevalier, R. A. 2002, ApJ, 577, L5

Berger, E., Kulkarni, S. R., Frail, D. A., & Soderberg, A. M. 2003, ApJ, 599, 408

Björnsson, C.-I., & Fransson, C. 2004, ApJ, 605, 823

Branch, D., et al. 2002, ApJ, 566, 1005

Canizares, C. R., Kriss, & Feigelson, E. 1982, ApJ, 253, L17

Chevalier, R. A. 1982a, ApJ, 258, 790

Chevalier, R. A. 1982b, ApJ, 259, 302

Chevalier, R. A. 1983, ApJ, 272, 765

Chevalier, R. A. 1998, ApJ, 499, 810

Chevalier, R. A. 2005, ApJ, 619, 839

Chevalier, R. A., & Fransson, C. 1994, ApJ, 420, 268

Chevalier, R. A., & Fransson, C. 2003, in Supernovae and Gamma-Ray Bursts, ed. K. W. Weiler (Berlin: Springer), 171

Chevalier, R. A., Fransson, C., & Nymark, T. K. 2006, ApJ, 641, 1029

Chugai, N. N., & Chevalier, R. A. 2006, ApJ, 641, 1051

Dahlén, T., & Fransson, C. 1999, A&A, 350, 349

Ellison, D. C., & Reynolds, S. P. 1991, ApJ, 382, 242

Ellison, D. C., Berezhko, E. G., & Baring, M. G. 2000, ApJ, 540, 292

Fransson, C. 1982, A&A, 111, 140

Fransson, C., & Björnsson, C.-I. 1998, ApJ, 509, 861

Galama, T. J., et al. 1998, Nature, 395, 670

Immler, S., Pietsch, W., & Aschenbach, B. 1998, A&A, 336, L1

Immler, S., Wilson, A. S., & Terashima, Y. 2002, ApJ, 573, L27

Iwamoto, K., Nomoto, K., Hoflich, P., Yamaoka, H., Kumagai, S., & Shigeyama, T. 1994, ApJ, 437, L115

Iwamoto, K., et al. 1998, Nature, 395, 672

Iwamoto, K., et al. 2000, ApJ, 534, 660

Jun, B.-I., & Norman, M. L. 1996, ApJ, 465, 800

Kouveliotou, C., et al. 2004, ApJ, 608, 872

Koyama, K., Petre, R., Gotthelf, E. V., Hwang, U., Matsuura, M., Ozaki, M., & Holt, S. S. 1995, Nature, 378, 255

Kulkarni, S., & Fox, D. W. 2003, IAUC No. 8073

Kulkarni, S. R., et al. 1998, Nature, 395, 663

Li, Z.-Y., & Chevalier, R. A. 1999, ApJ, 526, 716

Malesani, D., et al. 2004, ApJ, 609, L5

Matheson, T., et al. 2003, GCN No. 1846

Matzner, C. D., & McKee, C. F. 1999, ApJ, 510, 379

Mazzali, P. A., Iwamoto, K., & Nomoto, K. 2000, ApJ, 545, 407

Mazzali, P. A., et al. 2002, ApJ, 572, L61

Nugis, T., & Lamers, H. J. G. L. M. 2000, A&A, 360, 227

Paczyński, B. 2001, Acta Astronomica, 51, 1

Panagia, N., Sramek, R. A., & Weiler, K. W. 1986, ApJ, 300, L55

Panaiteescu, A., & Kumar, P. 2002, ApJ, 571, 779

Pelle, J.-C. 2004, <http://www.astrosurf.com/snweb2/2001/01ig/01igCurv.htm>

Pian, E., et al. 2000, ApJ, 536, 778

Pooley, D., & Lewin, W. H. G. 2003, IAU Circ., 8110, 2

Rodriguez Pascual, P., et al. 2002, IAUC No. 7821

Reynolds, S. P. 1998, *ApJ*, 493, 375

Richmond, M. W., et al. 1996, *AJ*, 111, 327

Ryder, S. D., Sadler, E. M., Subrahmanyam, R., Weiler, K. W., Panagia, N., & Stockdale, C. 2004, *MNRAS*, 349, 1093

Schlegel, E. M., & Ryder, S. 2002, *IAU Circ.*, 7913, 1

Soderberg, A. M., Nakar, E., Berger, E., & Kulkarni, S. R. 2006, *ApJ*, 638, 930

Soderberg, A. M., et al. 2003, GCN No. 1834

Soderberg, A. M., Chevalier, R. A., Kulkarni, S. R., & Frail, D. A. 2006, *ApJ*, submitted (astro-ph/0512413)

Soderberg, A. M., Kulkarni, S. R., Berger, E., Chevalier, R. A., Frail, D. A., Fox, D. B., & Walker, R. C. 2005, *ApJ*, 621, 908

Stanek, K. Z., et al. 2003, *ApJ*, 591, L17

Stockdale, C. J., Van Dyk, S. D., Weiler, K. W., Panagia, N., Sramek, R. A., Paczyński, B., & Rupen, M. P. 2003, *BAAS*, meeting 203, #87.02

Stockdale, C. J., Van Dyk, S. D., Sramek, R. A., Weiler, K. W., Panagia, N., Rupen, M. P., & Paczynski, B. 2004, *IAU Circ.*, 8282, 2

Stockdale, C. J., Sramek, R. A., Weiler, K. W., Van Dyk, S. D., Panagia, N., Montes, M. J., & Rupen, M. P. 2005, in *Cosmic Explosions: On the 10th Anniversary of SN 1993J* (IAU Coll. 192) Suppl., Eds, J. M. Marcaide & K. W. Weiler (Berlin: Springer), Poster 11

Suntzeff, N. B. 2003, in *From Twilight to Highlight: The Physics of Supernovae*, ed. W. Hillebrandt & B. Leibundgut (Berlin: Springer), 183

Sutaria, F. K., Chandra, P., Bhatnagar, S., & Ray, A. 2003, *A&A*, 397, 1011

Tan, J. C., Matzner, C. D., & McKee, C. F. 2001, *ApJ*, 551, 946

Tully, R. B., & Fisher, J. R. 1988, *Catalog of Nearby Galaxies* (Cambridge: CUP)

Timmes, F. X., Woosley, S. E., Hartmann, D. H., & Hoffman, R. D. 1996, *ApJ*, 464, 332

Tuthill, P. G., Monnier, J. D., & Danchi, W. C. 1999, *Nature*, 398, 487

Van Dyk, S., Sramek, R. A., Weiler, K. W., & Panagia, N. 1993, *ApJ*, 409, 162

Warren, J. S., et al. 2005, *ApJ*, 634, 376

Waxman, E. 2004, *ApJ*, 605, L97

Weiler, K. W., Sramek, R. A., Panagia, N., van der Hulst, J. M., & Salvati, M. 1986, *ApJ*, 301, 790

Wellstein, S., & Langer, N. 1999, *A&A*, 350, 148

Young, T. R., Baron, E., & Branch, D. 1995, *ApJ*, 449, L51

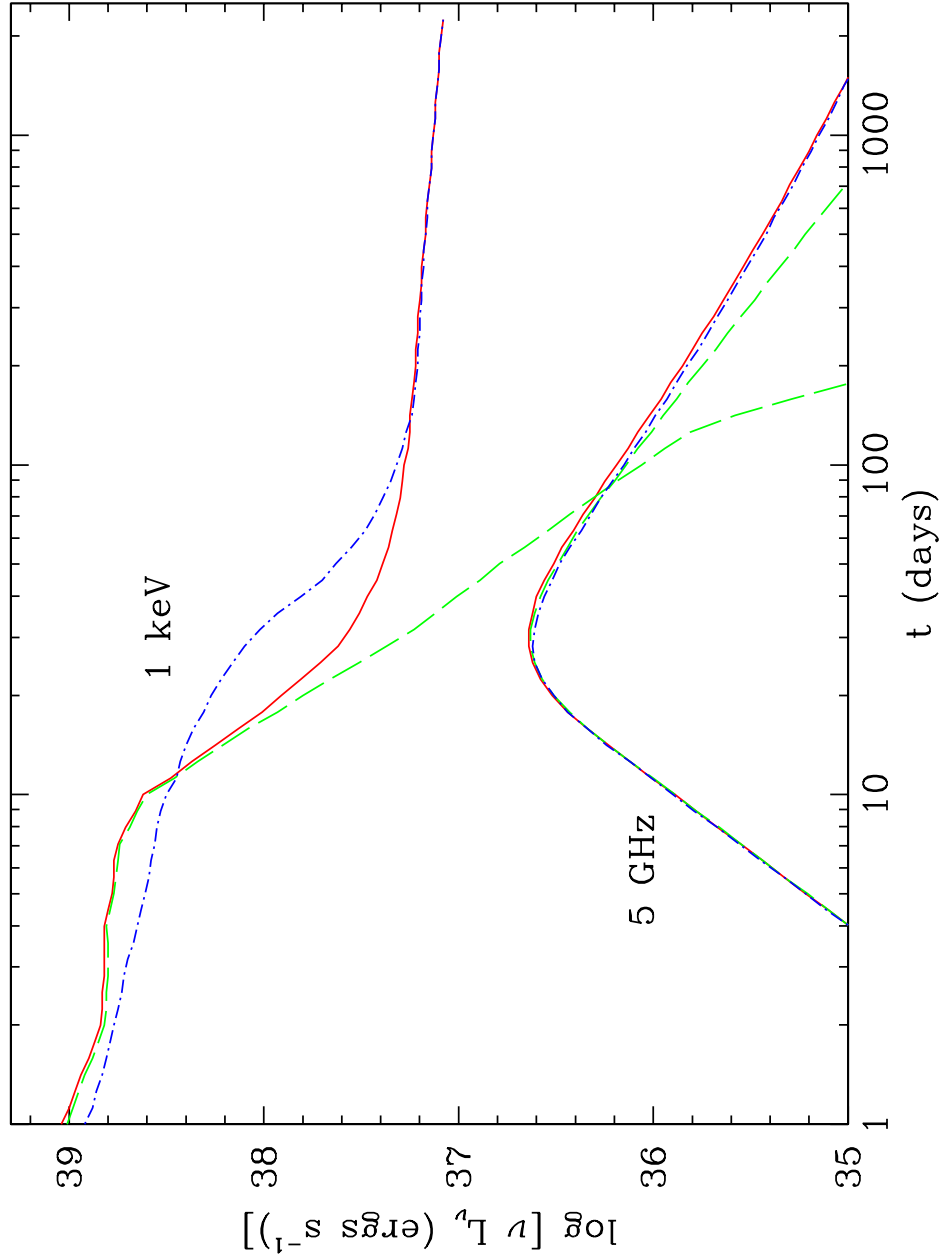


Fig. 1.— Model radio and X-ray light curves, including synchrotron and inverse Compton radiation. The green curve (*dashed line*) has a power law injection particle spectrum with  $p = 3.1$  and assumes an optical light curve like that of SN 1994I. The red curve (*solid line*) has an injection spectrum based on acceleration in a cosmic ray dominated shock and assumes a supernova like SN 1994I. The blue curve (*dashed-dot line*) is the same as the red, but assumes a supernova like SN 1997ef.

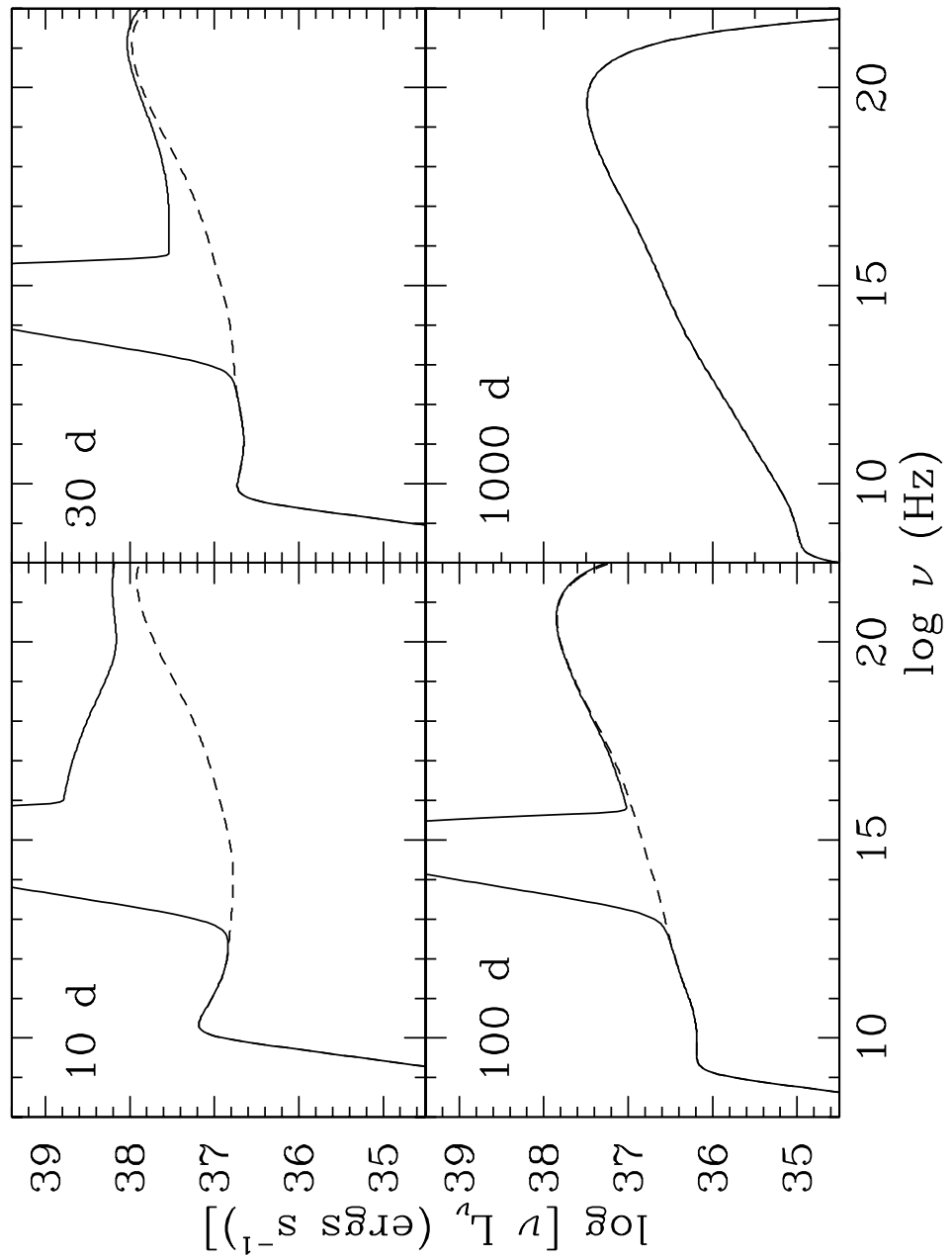


Fig. 2.— Selected spectra for an injection spectrum based on acceleration in a cosmic ray dominated shock and a supernova like SN 1994I. The dashed line shows the synchrotron component.